

A prospective study analyzing the application of radiofrequency energy and high-voltage, ultrashort pulse duration electrical fields on the quantitative reduction of adipose tissue

Diane Irvine Duncan¹, Theresa H. M. Kim², and Robbin Temeat¹

¹Plastic Surgery, Plastic Surgical Associates of Fort Collins, P.C., Fort Collins, CO, USA; ²Department of Family and Community Medicine, University of Toronto, Toronto, Ontario, Canada

ABSTRACT

Noninvasive fat reduction is claimed by many device manufacturers, but proof of efficacy has been difficult to establish. This prospective study was designed to measure the reduction of fat thickness and actual volume reduction in 20 female patients treated with an external radiofrequency (RF) device. This device combines RF heat, suction coupled vacuum, and oscillating electrical pulses that induce adipocyte death over time. Patients underwent pre- and post-treatment and intercurrent measurements of weight, body mass index, ultrasonic transcutaneous fat thickness, and 2D and 3D Vectra photography with independent calculation of circumferential and volumetric change. Mean transcutaneous ultrasound thickness at reproducible points was 2.78 cm; at 1-month post-treatment, the mean fat thickness was 1.71 cm. At 3-month post-treatment, the mean fat thickness reduction was 39.6%. Vectra circumference measurements were taken at 10-mm intervals, with postural and breathing cycle control. Independent analysis of serial measurements from +60 to -70 mm showed mean abdominal circumference measurement of 2.3 cm. Mean abdominal volume loss was 202.4 and 428.5 cc at 1- and 3-month post-treatment, respectively. Scanning electron microscopy confirmed that permanent cell destruction was caused by irreversible electroporation. Pyroptosis appears to be the mechanism of action.

ARTICLE HISTORY

Received 25 June 2015
Accepted 13 January 2016

KEYWORDS

Permanent fat reduction; adipocyte apoptosis; skin tightening; radiofrequency electroporation; noninvasive body contouring; pyroptosis

Introduction

An average American is 36.6 years old and has a body mass index (BMI) of 28.1 (1). This statistic classifies most Americans as being overweight. The mean weight of the average 5'4" woman is 164 lb, while the average 5'9" man weighs 190 lb. Over the past two decades, there has been an epidemic of increasing obesity and obesity-induced medical disorders in North America and the Western countries (2–6). The increased incidence of generalized, and, more importantly, aesthetically displeasing, localized fat deposits has resulted in the rapid research, development, and commercialization of noninvasive body contouring systems (6–8).

While surgical solutions for fat reduction, such as liposuction and dermolipectomy, are clearly effective in achieving a long-term improvement for localized lipodystrophy, only one in ten patients will actually pursue a surgical procedure after considering all the treatment options (9). Many more patients are interested in and will follow through with less risky and less painful noninvasive alternatives (6–9). A very attractive aspect of the noninvasive fat reduction procedures is that many of these technologies have little perceived risk, with little to no “down” time. More importantly, some of the most popular current technologies will actually destroy fat cells, offering patients a permanent focal adipose reduction.

Noninvasive body contouring technologies can be classified by the energy source deployed, or by their effect on adipose tissue. When educating patients, a more easily understood classification is that of the effect on the fat cell itself: (i) short-term metabolic size reduction and (ii) the long-term effect resulting from permanent fat cell death. Some medical devices can cause temporary fat reduction—in which the adipocyte size is reduced, but the cell is not permanently damaged. More sophisticated devices can create permanent focal fat reduction, in which the adipocyte has been permanently destroyed through the noninvasive application of some form of energy or physical injury (6–8, 10).

When deciding upon a particular noninvasive body contouring treatment and technology option, the permanent, noninvasive reduction of fat is increasingly the more compelling proposition. Currently available technologies, with peer-reviewed articles confirming histologically noninvasive permanent fat cell destruction with long-term body contour reductions, include the following: thermal necrosis of adipose tissue using high-frequency focused ultrasound (HIFU) (Liposonix, Valeant, Montreal, Canada), pulsed focused ultrasound that cavitates adipose tissue nonthermally (UltraShape, Syneron Candela, Yokneam, Israel), cryolipolysis, or CoolSculpting (ZELTIQ, Pleasanton, California) which

CONTACT Diane Irvine Duncan  momsurg@aol.com  Plastic Surgery, Plastic Surgical Associates of Fort Collins, P.C., 1701 E Prospect Rd., Fort Collins, CO 80525, USA. Color versions of one or more of the figures in the article can be found online at <http://www.tandfonline.com/ijcl>

Published with license by Taylor & Francis © 2016 Diane Irvine Duncan, Theresa H. M. Kim, and Robbin Temeat

This is an Open Access article. Non-commercial re-use, distribution, and reproduction in any medium, provided the original work is properly attributed, cited, and is not altered, transformed, or built upon in any way, is permitted. The moral rights of the named author(s) have been asserted.

causes hypothermal-induced apoptosis, and radiofrequency (RF)-induced electroporation of the fat cell membrane by BodyFX (InMode Invasix, Yokneam, Israel) (6–8).

However, there are some limitations of the aforementioned commercially available noninvasive permanent fat reduction systems. One limitation is the inability of cavitation ultrasound, thermal HIFU and cryolipolysis to tighten soft tissue and skin while simultaneously reducing the fat. It infrequently leads to volume reduction, but the patients complain of soft tissue laxity. Another limitation with the ultrasound and cryolipolysis devices is the inability to deliver “custom contouring” of the patient’s focal fat collection due to the fixed size of treatment applicator. Neither broad surface areas nor small localized regions can be properly addressed when a fixed square or rectangular treatment region is the only choice.

Recently, the BodyFX (InMode Invasix, Yokneam, Israel), a suction coupled, bipolar multiple frequency, RF-based device, has been shown in peer-reviewed articles to create permanent fat destruction through the application of trains of high-voltage pulsed electrical current with ultrashort pulse duration. It has been proposed that BodyFX emits trains of very short, nano-second pulse duration high-voltage pulses (HVPs), which cause irreversible electroporation (IRE) of the adipocyte cell membrane, with subsequent adipocyte death. In addition, the BodyFX emits synchronous standard RF energy with bulk heating of the skin and soft tissue, leading to soft tissue tightening and subsequent skin surface area reduction due to accommodation of the overlying skin (7,8).

Various technologies including thermal HIFU, cavitation pulsed focused ultrasound, and hypothermic cryolipolysis all have peer-reviewed studies showing abdominal circumference reduction of between 2 and 4 cm (6). However, there is no study to date which attempts to accurately measure the volume of fat reduction following permanent adipocyte injury caused by noninvasive treatments. This article reports the independently measured fat volume reduction in a prospective cohort of 17 patients, each of whom underwent 8 weekly BodyFX treatments. In addition, the study introduces scanning electron microscopy (SEM) histology, demonstrating the specific process of pyroptosis caused by IRE.

Materials and methods

Twenty qualified sequential female patients seeking noninvasive fat reduction in the abdominal region were included in this prospective study. Randomization of treatment location was not performed, as an accurate unilateral measurement could not be performed due to possible diffusion of the treatment effect across the midline. Inclusion criteria included an age limitation of 18–65 years, a BMI range of 18–32, a nonpregnant and nonlactating status, and a localized abdominal lipodystrophy not previously treated with any modality. Patients ranged in age from 19 to 62 years. Mean patient age was 41.71 years. Average height was 166.47 cm, and mean weight pre-treatment was 151.53 lb. Average BMI before treatment was 24.62.

Each patient was weighed prior to each treatment, and at each evaluation session. The weight of patients was tightly controlled in order to reduce its influence as a variable. While the mean

cohort weight was 151.53 lb prior to treatment, it was 150.2 one month following the final treatment. At 3 months, mean patient weight was 153.4 lb.

Qualified patients underwent eight weekly standardized treatments using the BodyFX with external RF heating of the skin and soft tissue to the therapeutic endpoint of 42°C, followed by the application of trains of ultrashort, high-voltage (2KV) RF pulses for 10 minutes in each abdominal quadrant. The entire abdomen was treated, divided into two epigastric quadrants and two infraumbilical quadrants.

Exclusion criteria

Exclusion criteria included an inability to maintain body weight within five pounds of the original measured weight for the duration of the study, inability to receive weekly treatments, an open sore in the treatment region, chronic medical condition that might impair healing such as diabetes, and an inability to follow up all post-treatment appointments. Patients were counseled not to change any current diet or exercise plans in an effort to eliminate these as variables.

Risks of treatment reviewed with each patient prior to treatment included little to no improvement in fat thickness, the perception of no result, asymmetry or unevenness, prolonged bruising or swelling, prolonged erythema, a burn, skin discoloration or pigmentation, and prolonged discomfort or dysesthesia.

Three patients were excluded from the study after enrollment. Two patients were forced to exit the study due to weight gain or loss of over five pounds from the initial study weight, and one did not return for the final evaluation at three months.

Procedure

The BodyFX is manufactured by Invasix (Yokneam, Israel). The device is approved by U.S. Food and Drug Administration (FDA) for the temporary reduction of cellulite (Figure 1).

All study patients were informed of the off-label use of the RF device. The BodyFX device employs a handpiece attached to the RF generator. The area of focal fat collection to be treated was marked out on the skin while the patient was standing.



Figure 1. The suction coupled, bipolar handpiece of the BodyFX.

The treatment was initiated by placing the handpiece firmly on the area of skin and soft tissue to be treated. When activated, the handpiece generates suction so that the tissue is drawn into the device's treatment region (Figure 2). The parameters of the device can be altered or adjusted. These adjustments include the power or energy in watts, the pulse duration, or number of seconds the suction coupled bipolar RF is applied, as well as the intensity of the "second RF," or how many "trains" of ultrashort, high-voltage electroporation RF pulses are released. The device is activated by pressing a foot pedal, which will result in activation of the suction and release of basic RF and the HVPs.

The BodyFX handpiece has an external temperature monitor that continuously reads the skin temperature. The device will control the release of the basic RF when the target therapeutic temperature of 41–43° is reached. At target temperature, the basic tissue heating aspect is turned off. When the temperature drops 0.1°C below the target temperature, RF heating is automatically turned back on again. This temperature-controlled RF delivery ensures that the skin and adipose tissue is automatically maintained at the therapeutic thermal endpoint. The "second RF" or the trains of HVPs are continuously released, regardless of the first RF or skin and soft tissue temperature. When the pulse duration is finished, the suction and RF emission are stopped, and the handpiece is moved to an adjacent skin and soft tissue area with approximately 20% overlap.

Marking of each patient prior to each treatment was performed in the upright position. The points of greatest protuberance of the focal abdominal adipose convexity were marked with a highlighter, and were noted on the treatment record for further reference.

In order to standardize treatment, each patient's abdomen was divided into four treatment quadrants. The upper left quadrant was labeled quadrant #1. The left lower quadrant was #2, the right lower quadrant was labeled #3, and right upper quadrant was labeled #4. No skin prep or gel was used during these treatments. Patients presented with clean skin; no lotion or body powder was allowed. The treatment pattern was drawn with a marking pen, with the umbilicus at the center of the rectangular pattern. The quadrants in the epigastrium ended at the inferior costal margin. Rectangles in the lower abdomen ended at the suprapubic crease. Lateral margins were an extension of the anterior axillary line. The use of these landmarks

helped maintain consistency in treatments, while ensuring that the entire abdomen was treated.

The settings for the first treatment included a power setting of 40 watts, with a 41°C maximum temperature. Power settings remained constant throughout the treatment sessions. However, the pulse width and maximum skin temperature did vary, as did the intensity of the "2nd RF" or train of oscillating pulses (Table 1). The general pattern was an increase of pulse width and HVP intensity with every other treatment. Maximum skin temperature was raised to 42° early in the treatment course. Placement of the handpiece was at 90° to the skin surface. Moderate pressure was used in order to get a good "seal" and therefore an effective vacuum. Each subsequent handpiece placement had 20% overlap of the pattern of the previous one. While the handpiece was advanced in a clockwise manner, the external temperature monitor noted the skin temperature. Once the maximum skin temperature was reached, the 10-minute timer was started and the trains of 2nd HVP RF were continuous throughout the treatment for each quadrant, which measured about 10 × 15 cm. Patients noted that the sensation of the HVPs was a "surprise" or a pressure shock, but most did not feel this felt like an electric shock. Many equated it to a "hiccup" or a feeling of muscle stimulation.

Average time to reach the therapeutic temperature was approximately 1 minute. This varied according to the individual's abdominal fat thickness. In smaller patients, only 4–6 passes were needed to get to the optimal skin temperature.

The duration of each treatment was about 45 minutes, as each patient received two passes in each quadrant per session. Treatment of the first quadrant took about 15 minutes, as the initial tissue heating took a little longer than the subsequent areas, which had a diffusion effect from the adjacent quadrant. As treatments progressed and the area became smaller, treatment duration was slightly shorter. As fat thickness was clinically and measurably reduced, treatment near the ribs became more uncomfortable for patients, so the quadrants became slightly smaller as well.

Clinical endpoints were the generation of diffuse erythema in the treatment region, and a feeling of perceptible tissue warmth, while achieving the temperature guidelines prompted by the device for the full 10-minute durations with two passes.

Measurement parameters: Canfield Vectra. The Vectra 3D circumferential imaging system (Canfield, NJ) was used to take three-dimensional photograph-generated measurements before any treatment, immediately after the 4th and 8th treatments, 1 month following completion of treatment, and again at three months following cessation of treatments (see Figure 3). The

BodyFX mechanism of action

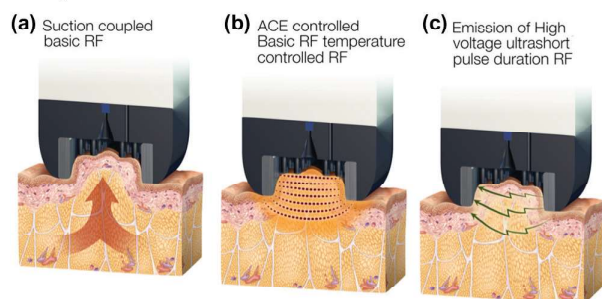


Figure 2. (a) The BodyFX handpiece is applied to the focal region. (b) Suction coupled, temperature-monitored basic RF for bulk tissue heating and skin tightening is applied. A thermistor and software algorithm will turn the RF energy off and on around the desired skin temperature. (c) Throughout the treatment cycle, using another frequency of RF, high-voltage (2 kV) pulses are continuously released with ultrashort, nanosecond pulse durations.

Table 1. Variation of settings with progression of 8 weekly treatments.

Treatment number	Pulse width	2nd RF intensity	Maximum skin temperature (°C)
1	2	2	41
2	2.5	2	41
3	3.0	3	42
4	3.5	3	42
5	3.5	4	42
6	4.0	4	42
7	4.5	5	42
8	5.0	5	42



Figure 3. The Vectra 3D scientific photographic station.

Vectra 3D photographs were controlled for inhalation and exhalation, as well as posture, at each timepoint. Serial Vectra measurements were evaluated by a computer technician using an algorithm based on serial circumference measurements taken 10 mm apart, as measured above and below the center of the umbilicus. The cylindrical segmental volumes were used to calculate the volume of the total as measured from +60 to minus 70 mm from the umbilical reference point (see Figure 4). Independent calculation of this volume at each time interval was performed by a Canfield technician, blinded to the study.

High-resolution ultrasound measurement of subcutaneous fat thickness. The thickness of abdominal subcutaneous tissue was measured at the same time intervals using a Philips high-resolution ultrasound device. Standardized measurement points were created at 1 cm lateral to the umbilical verge at the 12 o'clock, 3 o'clock, 6 o'clock, and 9 o'clock positions using an abdominal template. The distance from the basal dermis to Scarpa's fascia was measured using the Philips high-resolution machine at each of the four locations with a 15/2 linear array transducer at

these standardized points at each timepoint. Photographs of the cross-sections of abdominal fat were taken as well.

Scanning electron microscopy. In order to understand whether the device caused temporary egress of glycerol and triglycerides from the adipocyte leading to temporary adipocyte size reduction, or if the effects resulted in permanent cell destruction leading to a more permanent outcome, scanning electron microscopy (SEM) was performed in three volunteers at 2, 4, and 8 weeks after the treatment course was initiated.

Statistical Analysis of Results. Frequencies, means, and standard deviations for each characteristic were calculated (Table 2). Patients were categorized into four BMI groups: Underweight (BMI < 18.5), Normal (BMI 18.6–24.9), Overweight (BMI 25–29.9), and Obese (BMI 30+). Since “Underweight” and “Obese” categories had a cell count less than 5, the patients were further categorized into two groups: Underweight/Normal and Overweight/Obese. Independent and paired sample *t*-tests were computed to assess changes in pre-treatment and post-treatment scores. A repeated measures analysis of covariance (ANCOVA) was computed for the effects before and after treatment at five different timepoints for measuring abdominal subcutaneous thickness adjusted for the following covariates: age and BMI at baseline. Two-tailed significance level of 0.05 was used. All analyses were conducted using IBM SPSS 21.0.

Results. Expected side effects of the BodyFx treatments included temporary erythema, temporary discomfort, or minor swelling. Three patients noted the sensation of uncomfortable heat in the treatment region, which was immediately improved with the application of cool compresses.

Unexpected side effects—temporary problems which would resolve without further treatment—were experienced by one patient. She had mild petechiae in the treatment region lasting 48 hours after one treatment session. There were no thermal injuries; no burns were seen. Complications, defined as those unexpected side effects that might require further intervention, were not seen.

Pain and discomfort during treatment was reported as “tolerable” by all patients. All completed eight treatments, while noting their increasing tolerance to higher settings of pulse width and HVP RF. Thinner patients noted discomfort near bony prominences such as the rib or iliac crest as treatments progressed. None stated that the feeling of discomfort experienced was significant enough to deter them from receiving further treatments.

All seventeen patients who completed the study perceived an improvement in body contour. Some did not fully appreciate the change until 2D photographs were taken and reviewed. All patients observed a significant decrease in subcutaneous thickness as measured by the high-resolution ultrasound. No patient noted a perceptible visible contour change until after the 4th treatment.

Patients' comments included noting that clothing fit better or was looser than before treatment, and that soft tissue “jiggled less” while at the gym or in yoga class. No patient noted an increase in soft tissue laxity; twelve noted that their skin and soft tissue felt firmer and tighter. No patient noted a demarcation at

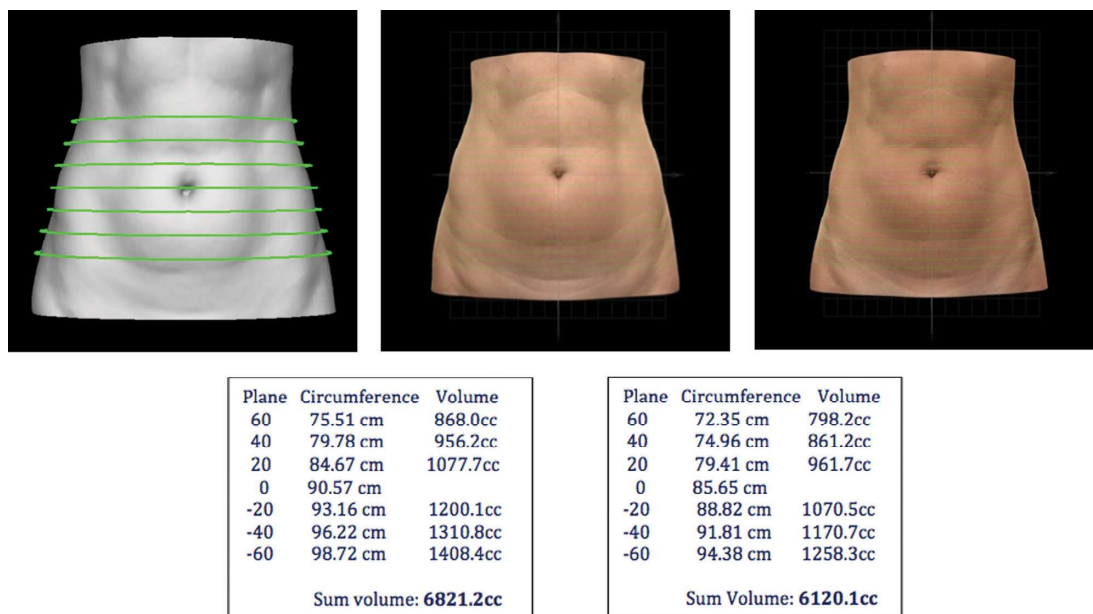


Figure 4. Vectra 3D measurements taken at intervals were evaluated by a computer technician using an algorithm based on serial circumference measurements taken 10 mm apart, as measured above and below the center of the umbilicus. The cylindrical segmental volumes were used to calculate the volume of the total as measured from + 60 to minus 70 mm. This patient had an abdominal fat volume reduction of 701cc.

the “edges” of their treatment region. None noted burns, prolonged bruising, or changes in skin pigment. While all patients saw improvement, three patients stated that they would like to have had more treatment sessions as the level of improvement was less than ideal. Two of these patients noted that surgical intervention such as liposuction might be more effective for the amount of fat reduction they felt would be optimal. Standard photographs showed visible improvement in all but subject 19, who gained twelve pounds during the treatment weeks. Parameters evaluated were abdominal protrusion, skin laxity, skin texture, improvement of pendulosity, and appearance of bra

roll (not treated). All patients who completed the study noted improvements in all five categories.

3D Vectra photographs were used for measurement. In order to better standardize comparative volume and circumference measurements, the upper limit of analysis was plus 60 cm above the central umbilical reference point. The lowest circumference measurement was taken at minus 70 cm. Limitations of this restriction meant that in taller patients, the entirety of the treated abdomen was not evaluated nor subjected to volumetric analysis, so in these patients some fat loss went unmeasured.

Table 2. Characteristics of patients.

Subject No.	Age (Years)	Pre-Tx weight (lbs)	Post-Tx weight (lbs)	Pre-Tx BMI	Pre-BMI category	Post-Tx BMI	Post-BMI category	Total volume change
1	57	151.0	150.8	24.4	Normal	24.3	Normal	71.2
2	57	149.0	157.0	24.8	Normal	26.1	Overweight	+ 162.3
3	34	118.0	115.0	21.6	Normal	21.0	Normal	601.9
4	33	135.0	138.8	21.1	Normal	21.7	Normal	241.9
6	45	156.0		26.0	Overweight			+ 99.2
7	38	112.5	115.0	18.2	Underweight	18.6	Normal	381.8
8	48	149.0	146.0	23.3	Normal	22.9	Normal	222.8
9	62	151.0	152.0	26.7	Overweight	26.9	Overweight	+ 154.8
10	22	130.0	122.0	23.0	Normal	21.6	Normal	1285.7
11	37	223.0	228.0	31.1	Obese	31.8	Obese	133.7
13	42	176.0	176.0	26.8	Overweight	26.8	Overweight	+ 392.9
14	19	176.0	178.0	27.6	Overweight	27.9	Overweight	513.9
15	49	164.5	171.0	26.5	Overweight	26.8	Overweight	+ 317.0
16	52	127.0	127.0	22.5	Normal	22.5	Normal	246.8
17	45	179.5	179.0	29.0	Overweight	28.9	Overweight	2.3
18	57	156.5	156.0	24.5	Normal	24.4	Normal	236.4
20	24	142.0	137.0	22.9	Normal	22.1	Normal	604.0
MIN	19	112.5	115.0	18.2		18.6		+ 392.9
MAX	62	223.0	228.0	31.1		31.8		1285.7
MEAN	41.9	151.8	151.9	24.7		24.6		199.9

(+) Indicates weight gain/fat volume gain. All other total volume change indicates weight loss.

The individual characteristics of 17 patients who underwent noninvasive fat reduction procedure are shown. The numbers were derived from Canfield Vectra M4–360 Body Imaging System, which measures circumference sectional volume (cc) of abdomen at different planes (e.g., 60 mm above umbilicus). Age, weight before treatment (lbs), weight after treatment (lbs), BMI before treatment, BMI after treatment, and total fat volume change are shown.

Table 3. Overall group mean change of circumference measurement of abdomen at each plane—before treatment and after treatment at 1 month, and at 3 months ($N = 17$ females).

Plane	Before treatment Mean \pm SD	After 1 month Mean \pm SD	After 3 months Mean \pm SD	Δ CHANGE 1 month	Δ CHANGE 3 months
+ 60	85.53 \pm 12.21	84.86 \pm 11.86	81.18 \pm 11.04*	0.67	1.42
+ 50	86.91 \pm 12.36	85.90 \pm 12.40	82.07 \pm 11.60*	1.01	1.89
+ 40	88.53 \pm 12.26	87.24 \pm 12.64*	83.40 \pm 12.02*	1.30	2.32
+ 30	90.25 \pm 12.06	88.83 \pm 12.71*	85.08 \pm 12.26*	1.43	2.61
+ 20	91.95 \pm 11.79	90.56 \pm 12.65*	86.90 \pm 12.37*	1.38	2.73
+ 10	93.53 \pm 11.44	92.28 \pm 12.50*	88.78 \pm 12.36*	1.25	2.71
+ 0	95.24 \pm 11.21	94.17 \pm 12.45	90.94 \pm 12.43*	1.07	2.52
- 10	96.47 \pm 10.93	95.56 \pm 12.26	92.36 \pm 12.30*	0.90	2.39
- 20	97.55 \pm 10.93	96.73 \pm 12.28	93.51 \pm 12.30*	0.82	2.27
- 30	98.69 \pm 11.01	97.91 \pm 12.29	94.66 \pm 12.31*	0.77	2.16
- 40	99.69 \pm 11.07	98.99 \pm 12.31	95.66 \pm 12.33	0.70	2.08
- 50	101.02 \pm 12.14	100.43 \pm 13.51	97.24 \pm 14.15	0.60	1.34
- 60	99.46 \pm 12.62	98.75 \pm 14.35	97.43 \pm 15.20	0.71	1.81
- 70	97.92 \pm 10.26	97.16 \pm 12.13	94.07 \pm 11.52	0.76	2.23
SUM OF CHANGE				14.76 cm At 14 sites	32.30 cm at 14 sites

The average means of $N = 17$ patients who underwent noninvasive fat reduction procedure are shown. The numbers were derived from Canfield Vectra M4-360 Body Imaging System, which measures circumference (mm) of abdomen at different planes. The change scores are derived from three timepoints: Before treatment, after treatment at 1 month, and after treatment at 3 months. The overall group mean indicates that on average, there was a total of 14.76-mm circumference reduction at 1 month and 32.30-mm circumference reduction at 3 months following the final BodyFX treatment. Mean change per measurement site was 1.05 cm at one month and 2.36 cm per site at three months post-treatment.

* $p < 0.05$.

Scientific measurements were calculated by an independent technician who was blinded to the study.

Evaluation of serial circumference measurements (Table 3) showed the sum of changes at fourteen locations rather than the traditional single, hand-held measuring tape measurement taken approximately at the level of the umbilicus. The mean circumference reduction of 1.34–2.73 cm at each point was calculated using a much more detailed and reproducibly accurate measurement system than a person using a hand-held measuring tape. At one month following treatment cessation, mean torso circumference reduction per measurement point was 1.054 cm. Interestingly, at three months, the serial circumference

measurements showed a mean reduction of 2.307 cm with no further treatments.

The individual volume of each 10-mm segment was calculated by the Canfield technician for each measured timepoint. Simple addition of these segmental volumes at each timepoint was used to calculate the comparative volumes as measured between + 60 and - 70 cm from the umbilical reference point. Table 4 shows the mean volumetric change of each volumetric unit with standard deviations. There was a range of segmental volumetric loss from 20.01 cc to 34.99 cc at 3 months following treatment. At 1-month post-treatment, mean total volumetric change was minus 202.36 cc. Three months after

Table 4. Overall group mean change of sectional volume measurement of abdomen at each plane—before treatment, after treatment at 1 month, and at 3 months ($N = 17$ females).

Plane	Before treatment Mean \pm SD	After 1 month Mean \pm SD	After 3 months Mean \pm SD	Δ CHANGE 1 month	Δ CHANGE 3 months
+ 60	563.11 \pm 161.51	551.83 \pm 159.85	501.91 \pm 144.51*	11.29	20.21
+ 50	582.24 \pm 165.26	567.47 \pm 166.26	515.27 \pm 151.47*	14.77	24.96
+ 40	603.55 \pm 166.63	586.77 \pm 170.48	533.35 \pm 157.22*	16.78	29.37
+ 30	625.74 \pm 167.00	608.45 \pm 173.68*	554.57 \pm 162.09*	17.29	32.65
+ 20	646.98 \pm 165.09	629.95 \pm 175.47*	576.84 \pm 165.78*	17.03	35.14
+ 10	665.90 \pm 162.95	649.73 \pm 175.24*	598.35 \pm 168.41*	16.17	36.45
+ 0	684.28 \pm 161.13	669.86 \pm 176.28	619.70 \pm 171.11*	14.42	36.01
- 10	705.69 \pm 162.52	693.06 \pm 179.71	642.68 \pm 174.41*	12.63	34.99
- 20	726.46 \pm 165.19	714.89 \pm 183.12	663.56 \pm 177.50*	11.57	34.05
- 30	744.74 \pm 168.27	733.99 \pm 186.84	680.95 \pm 180.13*	10.75	33.10
- 40	767.52 \pm 187.38	757.12 \pm 208.38	705.36 \pm 206.90	10.41	20.01
- 50	744.94 \pm 198.47	733.58 \pm 225.93	710.90 \pm 225.38	11.36	26.21
- 60	720.53 \pm 162.29	707.74 \pm 192.07	655.52 \pm 155.35	12.79	33.88
- 70	727.03 \pm 126.12	701.93 \pm 147.65	687.93 \pm 160.39	25.10	31.43
SUM OF CHANGE				202.36 cc	428.46 cc

The average means of $N = 17$ patients who underwent noninvasive fat reduction procedure are shown. The numbers were derived from Canfield Vectra M4-360 Body Imaging System, which measures sectional volume (cc) of abdomen at different planes. The change scores are derived from three timepoints: Before treatment, after treatment at 1 month, and after treatment at 3 months. The overall group mean indicates that on average, there was a total of 202.36-cc volume reduction at 1 month, and 428.46-cc volume reduction from abdomen at 3 months following the final BodyFX treatment.

* $p < 0.05$.

Table 5. Overall study participants fat reduction treatment results. Vectra 3D ultrasound abdomen thickness measurement (cm).

	Before treatment Mean \pm SD	After 1 month Mean \pm SD	After 3 months Mean \pm SD
Bivariate analysis			
US at 12 o'clock	2.72 \pm .892	1.84 \pm .667**	1.73 \pm .714**
US at 3 o'clock	2.90 \pm .563	1.64 \pm .533**	1.56 \pm .658**
US at 6 o'clock	2.68 \pm .853	1.83 \pm .661**	1.84 \pm .779**
US at 9 o'clock	2.81 \pm .727	1.55 \pm .503**	1.58 \pm .702**
Repeated measures ANCOVA			
US at 12 o'clock	2.63 \pm .283	1.74 \pm .202**	1.68 \pm .218**
US at 3 o'clock	2.83 \pm .160	1.57 \pm .164**	1.55 \pm .188**
US at 6 o'clock	2.60 \pm .249	1.71 \pm .184**	1.76 \pm .204**
US at 9 o'clock	2.82 \pm .237	1.49 \pm .150**	1.57 \pm .179**

The repeated measures ANCOVA has been adjusted for the following variables: Age (years) and height (cm). Overall group means of abdominal subcutaneous thickness as measured from the basal dermis to Scarpa's fascia at the same locations, measured at 1 cm from the umbilical verge at 12 o'clock, 3 o'clock, 6 o'clock, and 9 o'clock, are shown. US = ultrasound.

* $p < .05$; ** $p < .001$.

treatments ceased, the measured volume reduction averaged 428.46cc.

Ultrasound fat thickness measurements. Table 5 shows overall group means of abdominal subcutaneous thickness as measured from the basal dermis to Scarpa's fascia at the same locations—measured 1 cm from the umbilical verge at 12 o'clock, 3 o'clock, 6 o'clock, and 9 o'clock. Measurements were taken before any treatment, immediately following the 4th and 8th treatments, and at 1 month and 3 months following the final treatment. As measured by ultrasound, mean subcutaneous fat thickness in all locations before treatment was 2.78 cm. One month following the final treatment, the mean fat thickness was 1.71 cm. The mean subcutaneous thickness reduction measured as 1.06 cm at 1 month, and 1.10 cm at 3 months following the final BodyFX treatment. The mean reduction in adipose thickness was 39.6%.

Microscopic changes—SEM. Three patients volunteered for biopsies during and after their treatment to document any ultrastructural changes that might be happening to the adipocytes exposed to RF heat plus trains of ultrashort, high-voltage RF. While traditional histology performed on biopsies may show cell wall disruption (necrosis) or silent cell death with special stains (apoptosis), the process of pyroptosis can be better understood by evaluating the changes in cellular structure over time with SEM.

A normal adipocyte in the untreated control region shows the uniform texture of the cell wall with a spongy intact cell membrane (Figure 5a). At two weeks post-treatment, adipocytes in the treatment region show regions of focal delamination (Figure 5b). Four weeks after the RF treatment, combined treatment of continuous RF heat plus HVPs was initiated; SEM shows cracks in the cell membrane with migration of fibrocytes (arrow) to the injured spot (Figure 5c). At eight weeks, immediately following the final treatment, significant volume reduction of the adipocytes is seen in clumps, or in what appears to be a fractional pattern (Figure 6a). Normal appearing, apparently unaffected adipocytes are located in an adjacent section. Isolated instances of cell disruption (Figure 6b) are noted, as

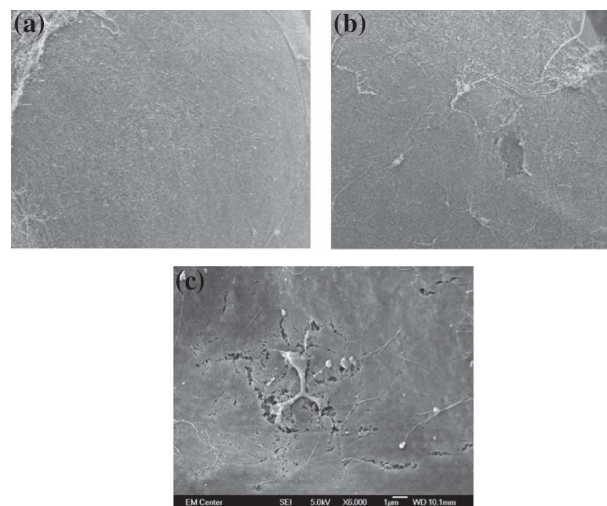


Figure 5. (a) Control: the untreated adipocyte cell membrane shows a smooth and spongy surface. (b) Adipocyte following two treatments with BodyFX. Note the small region of delamination of the cell wall. (c) Immediately after the fourth treatment, diffuse cracks in the outer membrane of the adipocyte are present. A fibrocyte has migrated to the region, marking the onset of an inflammatory response.

well as further delamination of the outer wall of the cell membrane. Multiple “pores” in the adipocyte membrane are created, large enough for tiny lipid droplets to pass through. The egress of lipid from the intracellular location causes significant volume loss, which is followed by signaled cell death.

Statistical analysis of results

Two methods of statistical analysis were applied for the data evaluation of the final 17-member cohort. Three characteristics were analyzed: the change in abdominal subcutaneous thickness as measured with high-resolution ultrasound, change in abdominal circumference at 14 levels including at the umbilicus as measured with the Canfield Vectra system, and volumetric change over time as measured with the Canfield Vectra system.

Independent and paired sample *t*-tests showed a *p* value of $< .05$. Repeated measures ANCOVA adjusted for differences in age, as well as height and weight (proxy for BMI) to minimize individual differences and control for extraneous variables that may affect the pre- and post-treatment results was analyzed. No confounding variables were found.

All analyses were conducted using IBM SPSS 21.0.

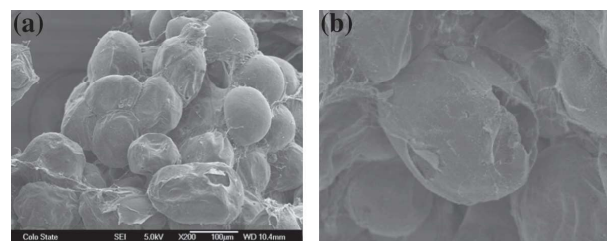


Figure 6. (a) Immediately following the eighth treatment, significant volume loss of clusters of adipocytes is seen. The response is fractional, as some adipocytes on the right appear undamaged. (b) Immediately following the eighth treatment, some adipocytes show frank rupture of the cell wall.

Discussion

Completely noninvasive solutions for lipodystrophy combined with skin laxity are highly sought after by aesthetic sector consumers. While the number of devices, injectables, and topicals claiming such attributes are a legion, few, if any, can demonstrate a scientifically sound basis for these claims. Device types that have proven to achieve permanent fat reduction include cryolipolysis, HIFU, and cavitational ultrasound (6,8). These devices employ expensive disposables, and treat only a rectangular-shaped region of lipodystrophy. The mechanism of action (MOA) with cryolipolysis is apoptosis, or silent cell death. With both types of ultrasound devices, the MOA is necrosis of a portion of a fixed depth of soft tissue in the treatment area's hypodermis. Neither device type has shown the ability to reduce fat thickness and tighten soft tissue and skin at the same time. Internal chemical adipose ablation, in the form of injection lipolysis, can cause soft tissue contraction (11). However, no FDA-approved injectable lipolytic is currently available in the United States.

Traditional suction-assisted lipectomy (SAL) is a well-regarded method for obtaining permanent fat reduction. However, a recent study (12) showed that SAL caused a skin surface area contraction of only about 10% at six weeks following treatment. At one year following SAL, this skin surface area reduction had relaxed to 8%. Many patients present with both preexisting skin laxity and lipodystrophy. Once a patient's subcutaneous volume is depleted, skin laxity, if untreated, becomes more pronounced. If the need for skin surface area reduction exceeds 8–10%, neither SAL nor currently popular noninvasive device treatments will achieve the patient's goals.

Thorough patient evaluation and communication are clearly the keys to success when choosing any treatment, whether it is surgical or noninvasive. As unmet expectations are a common cause of patient dissatisfaction in many aesthetic practices, it is important to understand the expected outcome before recommending a treatment plan. One study showed that only 10% of U.S. patients seeking improvement in body contour will follow through with surgery for an aesthetic complaint (9). The American Association of Aesthetic Plastic Surgeons statistics show a consistent uptrend in the number of minimally invasive and noninvasive procedures as compared to surgical procedures over the last ten years (13). However, patients seeking noninvasive solutions are oftentimes disappointed in the limited improvement achieved with these treatments. Patient considerations include downtime, cost, safety and efficacy, and the number of visits to the doctor's office needed to achieve a perceptible outcome, as well as the perceived risk of each treatment option.

RF heating, both internally and externally, has emerged as the most common bulk heater of skin and adipose tissue. (6,10,13–15). Sadick notes that RF energy is preferred over ultrasound, laser, or light-based technologies when skin and soft tissue contraction is a primary goal (16). While laser assisted lipectomy can create skin surface area reductions of up to 17% (18), radiofrequency assisted lipectomy generates a 26.4% skin surface area reduction at 6 weeks post-treatment (12), and a 35.4% measured skin surface contraction at one year. For many patients, permanent fat reduction alone will not achieve their optimal outcome. Soft tissue tightening, such as improvement

of the “muffin-top” phenomenon, is a frequently voiced goal. Skin surface area reduction and skin quality improvement are another common request.

Technologies based on apoptosis induction can generate long-term fat reduction. In the currently available form, cryolipolysis treatments take about an hour, and only a fixed treatment area size is available. Most regions of lipodystrophy are neither square nor rectangular. Most taper from a thinner fat deposit at the periphery to a convex peak at the center, and are more round or oval in shape. “Stampers” (17) are limited in treating individual fat deposits as no accommodation for individual variation can be made. “Movers”—devices with a movable handpiece and no fixed treatment size—can better accommodate variable sizes and depths of lipodystrophic fat deposits.

Since, by definition, apoptosis causes silent cell death (no inflammation), volume loss alone occurs with this MOA. In patients whose only concern is fat reduction, cryolipolysis is a good solution. However, for those patients with a pendulous region of lipodystrophy, or those with generalized accompanying skin laxity, a device with a different MOA would be more optimal.

Both HIFU and cavitational ultrasound-based fat reduction have been shown to produce long-term results. These devices are also “stampers,” and only treat a fixed area of fatty tissue, regardless of the patient's size or degree of lipodystrophy. HIFU is painful, and multiple treatment sessions are needed in order to obtain optimal results. As these device types have an inability to customize the treatment—to use more energy in regions that need more fat reduction or tissue tightening—a flat or “boxy” look can be the result. Since necrosis of 1.5 cm of the subcutaneous layer in a rectangle is the result of treatment with HIFU, significant inflammation and scarring can be created in the focal treatment region. Overlying soft tissue can be tethered by scar tissue to the underlying fat and fascia, and the ability of the soft tissue to glide over the underlying bone and muscle can be impaired. Too much scar tissue formation in a fixed treatment region may cause a tell-tale deformity afterwards. Ideally, a noninvasive fat-reducing treatment would generate a fractional soft tissue response along with mild but diffuse neocollagenesis, which would cause fibroseptal network contraction with accommodation and shrinkage of the overlying skin.



Figure 7. (a) A 23-year-old subject before noninvasive RF treatment with BodyFX. Result at 3 months following 8 treatments. (b) A 62-year-old subject with pendulous abdominal lipodystrophy. Result at 3 months. Definite improvement is seen, but skin laxity has not been fully corrected. Note improvement of bra roll and flanks; these regions were not treated.



Figure 8. A 44-year-old subject with generalized abdominal lipodystrophy. Result at 3 months following 8 treatments with noninvasive RF device. Vectra measurements showed 701-cc fat loss.

Externally applied noninvasive RF is a popular energy source for bulk dermal and adipose tissue heating. RF devices come in many configurations, including monopolar (Thermage and Pelleve), bipolar (VelaShape), and multipolar (TriPollar, Venus Freeze, and Forma) iterations. (6–8, 13). The application of basic RF (one million cycles per second and low amplitude) has been well documented to stimulate new collagen formation and cause some skin tightening, but it generally does not cause permanent cell destruction.

The BodyFX is a unique noninvasive RF-based body contouring device as it synchronously deploys two different types of RF energy. This combination of energy patterns can cause permanent adipose tissue destruction, presumably through applied electrical fields across the fat cell membrane. Induction of IRE can cause cell death in up to 30% of the fat cells treated (6–8). Review of histological post-treatment changes as compared to biopsies taken prior to treatment showed compaction of the dermis with new collagen deposition in the dermis (7, 8). Clinical response with this RF treatment varies with the amount of fat present in the treatment region. Thinner patients generally see more dramatic improvement clinically than more obese patients (Figure 7a,b), as the finite amount of fat to be treated is less in volume. However, significant improvement was also noted in the overweight group as well (Figure 8).

IRE relies on the principles of bioelectrics. Bioelectrics is the basic science field of applied electrical fields to living systems and cellular function. Nonablative cellular thermal stimulation

has been shown in other nonmammalian and mammalian cell lines to lower the electroporation threshold (27). It has been shown that applying ultrashort, high-amplitude electrical fields to a cell membrane can reversibly or irreversibly change the polarity of that membrane, altering cell function and viability (18–26). By specifically tailoring the pulsed electrical field to the target tissue and ensuring that trains of ultrahigh amplitude, ultrashort pulse duration electrical fields are applied across a cell membrane and exceed the “recharging time” of that membrane, irreversible cell membrane injury can occur (19–27). *Reversible electroporation* is used in medicine to enhance penetration of molecules across cell membranes that are too large for normal physiologic transport (19). Generally, the duration of the pulsed electrical field in these reversible electroporation devices are long enough, with low amplitude so that there is no irreversible damage to the target cell membranes. However, the application of a series or train, of multiple, ultrashort (in the nanosecond pulse duration range) electrical pulses with very high amplitude—two kilovolts per pulse—across a cell membrane, such as an adipocyte, can result in irreversible damage to the exquisitely regulated phospholipid bilayer membrane proton pump systems. These keep the transmembrane potential and external environment positively charged with the calcium ions retained outside and the pH of the internal cellular adipocyte milieu tightly regulated (7,8,18–26). The irreversible change in the transmembrane potential changes the configuration of the cell membrane in affected adipocytes leading to the creation of pores, or openings in the cell membrane, allowing calcium, organic solutes, and inorganic ions to stream through the defects in the protective cell membrane. This process changes the chemical and structural milieu of the cytoplasm (Figure 9). “Rafts” of lipid droplets egress from the adipocyte through these pores, causing significant cellular volume loss followed by signaled cell death.

Initially, the mechanism of cell death caused by treatment with the BodyFX device was thought to be apoptosis, as the study by Boisnic and Divaris (7) showed histologic slides that stained positive for apoptotic bodies. However, since several elements

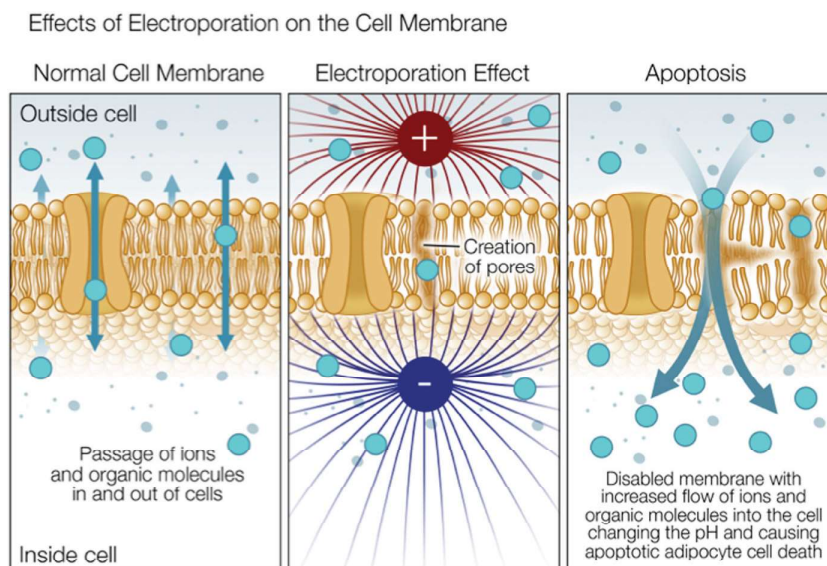


Figure 9. BodyFX creates an IRE effect on the cell membrane of the adipocyte, which over time leads to cell death. Basic RF heat may lower the IRE threshold.

of necrosis and apoptosis can overlap, more than one marker should be checked in order to positively identify the MOA (28). The mechanism of solely silent cell death through IRE does not adequately explain why soft tissue and some skin tightening is seen (Figure 10) following these treatments. While histology can show both necrosis and apoptosis fairly well, the elucidation of the complex pyroptotic response may be better seen with serial SEM specimens taken at progressive timepoints.

Pyroptosis, discovered by Dr. Brad Cookson (29), is a mechanism of cell death that exists in a space located somewhere between two polar opposites. Apoptosis (silent, signaled cell death) and necrosis, often referred to as “oncosis” (30) because of the invariable swelling response, have been thought to be the only answers to the riddle of how cells die for many years. Pyroptosis exhibits some elements of both cell death pathways.

Exhaustive research during the past decade (31–36) has uncovered many ways that cells respond to targeted attacks, whether the source is a microbe, a toxin, or a process inherently programmed by individual genetics. It is important to note the differences between methods of cell death as each has clinical advantages and limitations. As defined by Fink (37), the process of apoptosis is mediated by initiator caspases (2,8–10), and effector caspases (3,6,7). Samali (38) notes that the hallmarks of apoptosis include both condensation of the cytosol and nuclear contents of the cell, as well as creation of apoptotic bodies. This form of programmed cell death exhibits no loss of cell wall integrity. Autophagy is common, and inflammation is absent.

The term “necrosis” is commonly used to describe a method of cell death that involves lysis of the cell wall with egress of lysosomes from the cell, which causes immediate swelling, bleb formation, and subsequent failure of the ionic pumps across the lipid bilayer. Technically, the term is used to describe a cell that is already dead, so the term “oncosis” (30) is commonly used to describe the pathophysiologic process of active cellular demise. The process of oncosis is marked by definite and immediate inflammation due to cytoplasmic release into the extracellular space.

The process of pyroptosis is mediated by caspase 1 and sometimes caspase 11. This process is called “proinflammatory” because secretion of both cytokines interleukin (IL)-1 β and IL-8 are stimulated. Caspase 1 also causes “poration” of the cell membrane, with openings large enough to allow extracellular calcium inside the cell. Lysosomal and lipid droplets exit the cell, with depletion of cellular volume (39). Interestingly, noninfectious processes such as coronary ischemia, cerebrovascular accidents, and cancer can generate pyroptotic response in humans (40). Infectious agents such as *Salmonella*, anthrax bacteria, and *Legionella* can generate a pyroptotic response through different mechanisms (41). Since adipocytes are unique

in that intracellular lipid droplets abound, it is possible that the response of this tissue type to the RF-generated HVPs is tissue specific. SEM study showed intact dermal cells, fibrocytes, red blood cells, platelets, and white blood cells. The response to treatment is gradual and progresses over time, explaining why the reduction response appears to peak 3 months after the final RF treatment.

Advantages of treating patients with a device generating a pyroptotic MOA include creation of a fractional response similar to that of apoptosis, but with some inflammatory response, which can create a soft tissue and skin contraction due to the effect on the fibroseptal network. Since full necrosis is never generated, there is no downtime, as swelling is not a noted response. A more significant advantage is the lack of skin contour irregularities post-treatment, as the diffuse and mild inflammatory response does not cause enough focal fat loss to create depressions and protrusions. Since the fibrocytes respond to pyroptotic stimuli with less enthusiasm than to necrotic stimuli, the disadvantage of subcutaneous fibrosis with restriction of the gliding surface is avoided.

Study limitations. The measurement of success for noninvasive body contouring has been circumferential reduction (CR). However, CR is generally subject to wide inter-observer variability due to the subjective nature of the tape measurement itself, tensing or relaxation of the abdominal wall, postural variations, and inhalation–exhalation cycles. In this study, the use of an objective computerized measurement system with controls for breathing cycle and posture did reduce some of the human error generated by less sophisticated measurement systems. However, the transcutaneous measurement of the thickness of the subcutaneous fat can be subject to inter-observer variability resulting from variable pressure exerted on the ultrasound transducer when placed on the skin.

Treatment limitations. A limitation of treatment with BodyFX includes the need for multiple treatments one week apart, which can be difficult for patients who work and those traveling from a significant distance. In patients with soft, “pudding-like” fat, generally those with skin types I and II, the treatment seems to work very well. Dr. Henry Chan (42) noted that cryolipolysis works less well in the Asian population than in Caucasians, especially when more than one treatment is given. It is possible that noninvasive RF-based treatments for fat reduction may also be affected by ethnic differences in subcutaneous tissue. Noninvasive fat reduction treatments will not replace liposuction, as large volumes of fat reduction cannot be easily achieved. In patients with a significant amount of skin laxity, dermolipectomy remains the treatment of choice.

Conclusions

Application of temperature-controlled RF bulk heating plus trains of high-voltage, ultrashort pulse duration RF with the BodyFX once weekly for 8 weeks resulted in the following changes to the adipose tissue:

1. As measured by ultrasound, mean subcutaneous fat thickness before treatment was 2.78 cm. The mean subcutaneous thickness reduction was 1.10 cm at three months following



Figure 10. A 58-year-old subject before treatment with RF-based BodyFX. Result at 3 months following 8 treatments. Note improvement in cellulite.

the final BodyFX treatment. The mean reduction in adipose thickness was 39.6% three months following the final treatment.

2. Vectra 3D measurements show a mean abdominal circumferential reduction of 2.3 cm three months following the final treatment.
3. Vectra 3D measurements documented a 428.46-cc mean volume loss of fat at the 3-month timepoint.
4. SEM confirms that IRE with tears in the cell membrane followed by egress of lipid droplets and loss of cell volume appears to be the mechanism of permanent fat cell death.
5. RF-induced fat loss caused by electroporation-induced cell death generated a fractional tissue response with what appears to be a combination of fat loss and soft tissue tightening. However, obese patients and those with severe skin laxity are best treated with more traditional methods.

Declaration of interest

The device for the study was loaned by InMode. The authors alone are responsible for the content and writing of the report.

References

1. American Society of Aesthetic Plastic Surgery. Quick facts: 2013 ASAPS Statistics. Available at: <http://www.surgery.org/media/statistics>.
2. American Society of Aesthetic Plastic Surgery, 2013ASAPS statistics: complete charts (including percent change, gender distribution, age distribution, national average fees, practice profile). Available at: <http://www.surgery.org/media/statistics>.
3. Global aesthetic medicine VIII: the global aesthetic market study. Medical Insight Inc; 2013
4. Heart Disease News. "Waist size predicts heart disease risk better than BMI." 2008. Available at: www.healthhubs.net.
5. Wang Y, Beydoun MA. The obesity epidemic in the U.S.—gender, age, socioeconomic, racial/ethnic, and geographic characteristics: a systematic review & meta-regression analysis. *Epidemiol Rev*. 2007;29:6–28.
6. Mulholland RS, Paul MD, Chalfoun C. Non-invasive body contouring with radiofrequency, ultrasound, cryolipolysis, and low-level laser therapy. *Clin Plast Surg*. 2011;38:503–520.
7. Bojsnic S, Divaris M, Nelson AA, Gharavi NM, Lask GP. A clinical and biological evaluation of a novel radiofrequency device for the long-term reduction of adipose tissue. *Laser Surg Med*. 2014;46:94–103.
8. Mulholland RS, Kreindel M. Non-Surgical body contouring: Introduction of a new non-invasive device for long-term localized fat reduction and cellulite improvement using controlled, suction coupled, radiofrequency heating and high voltage ultra-short electrical pulses. *J Clin Exp Dermatol Res*. 2012;3(4):157–165.
9. Sound Surgical Vaser training presentation, April 14, 2005. Fort Collins, CO.
10. Paul MD, Mulholland RS. A new approach for adipose tissue treatment and body contouring using radiofrequency-assisted liposuction. *Aesth Plast Surg*. 2009;33(5):687–694.
11. Duncan DI, Rubin JP, Golitz L, Badylak S, Kesel L, Freund J, Duncan D. Refinement of technique in injection lipolysis based on scientific studies and clinical evaluation. *Clin Plast Surg*. 2009;36(2):195–209.
12. Duncan DI. Nonexcisional tissue tightening: creating skin surface area reduction during abdominal liposuction by adding radiofrequency heating. *Aesth Surg J*. 2013;33(8):1154–1166.
13. http://www.surgery.org/sites/default/files/Stats2013_4.pdf. Accessed 07-14-14.
14. Paul MD, Blugerman G, Kreindel M, Mulholland RS. Three-dimensional radiofrequency tissue tightening: A proposed mechanism and applications for body contouring. *Aesth Plast Surg*. 2011;35(1):87–95.
15. Mulholland RS. Radio frequency energy for non-invasive and minimally invasive skin tightening. *Clin Plast Surg*. 2011;38:437–448.
16. Sadick N. Tissue tightening technologies: fact or fiction. *Aesthet Surg J*. 2008;28(2):180–188.
17. Mulholland S. What's new in radiofrequency-based medical devices. IMCAS Asia 2014, Hong Kong, July 31, 2014.
18. Dibernardo BE. Randomized blinded split abdomen study evaluating skin shrinkage and skin tightening in laser-assisted liposuction vs. liosuction control. *Aesthet Surg J*. 2010;30:593–602.
19. Davalos M, Rubinsky B. Tissue ablation with irreversible electroporation. *Ann Biomed Eng*. 2005;33:223–231.
20. Schoenbach KH, Hargrave B, Joshi RP, Kolb JE, Nuccitelli R, Osgood C. et al. Bioelectric effects of intense nanosecond pulses. *IEEE Trans Dielectr Electr Insul*. 2007;14:1088–1090.
21. Schoenbach KH, Xiao S, Joshi RP, Thomas Camp J, Heeren T, Kolb JE, Beebe SJ. The effect of intense subnanosecond electrical pulses on biological cells. *IEEE Trans Plasma Sci*. 2008;36:414–422.
22. Rubinsky B, Onik G, Mikus P. Irreversible electroporation: a new ablation modality – clinical implications. *Technol Cancer Res Treat*. 2007;6:1–12.
23. Rubinsky B. Irreversible electroporation in medicine. *Technol Cancer Res Treat*. 2007;6:255–259.
24. Miller L, Leor J, Rubinsky B. Cancer cells ablation with irreversible electroporation. *Technol Cancer Res Treat*. 2005;4:1–7.
25. Onik G, Rubinsky B, Mikus P. Irreversible electroporation: implications for prostate ablation. *Technol Cancer Res Treat*. 2007;6:1–6.
26. Maor E, Ivorra A, Leor J, Rubinsky B. The effect of irreversible electroporation on blood vessels. *Technol Cancer Res Treat*. 2007;6:307–312.
27. Ohshima T, Okuyama k, Sato M. Effect of culture temperature on high-voltage pulse sterilization of *Escherichia coli*. *J Electrostatics*. 2002;55(3–4):227–235. DOI:10.1016/SO304-3886(01)00206.
28. Coll NS, Epple P, Dangle JL. Programmed cell death in the plant immune system. *Cell Death Diff* 2011;18:1247–1256.
29. Cookson BT, Brennan MA. "Pro-inflammatory programmed cell death". *Trends in Microbiology*. 2001;9(3):113–114.
30. Majno G, Joris I. 1995. Apoptosis, oncosis, and necrosis. An overview of cell death. *Am. J. Pathol*. 146:3–15.
31. Blagosklonny MV. Cell death beyond apoptosis. *Leukemia* 2000;14:1502–1508.
32. Ekert PG, Silke J, Vaux DL. Caspase inhibitors. *Cell Death Differ*. 1999;6:1081–1086.
33. Fantuzzi G, Dinarello CA. Interleukin-18 and interleukin-1 β : two cytokine substrates for ICE (caspase-1). *J. Clin. Immunol*. 1999;19:1–11.
34. Hueffer K, Galan JE. Salmonella-induced macrophage death: multiple mechanisms, different outcomes. *Cell Microbiol*. 2004;6:1019–1025.
35. Jaattela M. Programmed cell death: many ways for cells to die decently. *Ann Med* 2002;34:480–488.
36. LaRock CN, Cookson BT. Burning Down the House: Cellular Actions during Pyroptosis. *PLoS Pathog*. 2013;9(12):e1003793. doi:10.1371/journal.ppat.1003793.
37. Fink SL, Cookson BT. Apoptosis, pyroptosis, and necrosis: mechanistic description of dead and dying eukaryotic cells. *Infect immune*. 2005;73:1907–1916.
38. Samali A, Zhivotovsky B, Jones D, Nagata S, Orrenius S. Apoptosis: cell death defined by caspase activation. *Cell Death Differ*. 1999;6:495–496.
39. Bergsbaken T, Fink SL, den Hartigh AB, Loomis WP, Cookson BT. Coordinated Host Responses during Pyroptosis: Caspase-1-Dependent Lysosome Exocytosis and Inflammatory Cytokine Maturation. *J Immunol*. 2011;187:2748–2754.
40. Bergsbaken, Fink SL, Cookson BT. Pyroptosis: host cell death and inflammation. *Nat Rev Microbiol*. 2009;7(2):99–109.
41. Fink SD, Bergsbaken T, Cookson BT. Anthrax lethal toxin and salmonella elicit the common cell death pathway of caspase-1 dependent pyroptosis via distinct mechanisms. *Proc Natl Acad Sci U S A*. 2008;105(11):4312–4317.
42. Chan, HH. Personal comment, IMCAS Asia. Aug 2, 2014, Hong Kong.